Supplemental material

A. Supplemental Materials and Methods

B. Supplemental Figures

FIG S1 The well system for *in situ* bioremediation of U(VI) with EVO, showing groundwater flow direction and distribution of eight wells for this study.

FIG S2 Groundwater concentrations of acetate, U(VI), nitrate, sulfate, Mn(II), and Fe(II) in the eight wells before and after EVO amendment.

FIG S3 Hierarchical cluster analysis of all functional genes detected in the eight wells.

FIG S4 Average relative abundance of (a) representative genes involved in the degradation of organic carbon compounds and (b) genes for CO_2 fixation in seven downgradient wells (W1-W7) after EVO amendment.

FIG S5 Enrichment of key genes involved in acetongenesis, methanogenesis, and methane oxidation in the seven downgradient wells 17 days after EVO amendment.

FIG S6 Changes in the relative abundance of genes involved in N cycling in the seven downgradient wells after EVO amendment.

FIG S7 Enrichment of key genes involved in dissimilatory nitrate reduction in the seven downgradient wells 17 days after EVO amendment.

FIG S8 Enrichment of *dsrAB* genes encoding dissimilatory sulfite reductase in the seven downgradient wells after EVO amendment, showing EVO stimulation of *Desulfovibrio* and *Desulfotomaculum* species.

FIG S9 Changes of major cytochrome-containing populations in the seven downgradient wells after EVO amendment.

FIG S10 Changes in the composition and structure of cytochrome-containing communities in the seven downgradient wells after EVO amendment.

FIG S11 Enrichment of hydrogenase genes in the seven downgradient wells 17 days after EVO amendment.

FIG S12 Enrichment of metal resistance (a and c) and organic contaminant degradation (b and d) genes in the seven downgradient wells (W1-W7) at 17 days after EVO amendment.

C. Supplemental Table

Table S1 Significance of the effects of EVO amendment on community functional structure and concentrations of acetate and electron acceptors.

D. Supplemental References

A. Supplemental Materials and Methods

Site description. This study was performed in Area 2 of the US Department of Energy's Oak Ridge Integrated Field Research Challenge (ORIFRC) site, TN. The test plot is located about 300 m from the former S-3 waste ponds (the source of contamination). Contaminants in the groundwater (pH 6.6-6.9) were transported through the primary contaminant path and are primarily U (3.8-7.1 μM), sulfate (1.0-1.2 mM) and nitrate (0.2-1.5 mM) with up to $\geq$300 mg/kg U in soil-saprolite (14). Dissolved oxygen was near zero although oxygen can infiltrate into the upper vadose zone from the atmosphere. The groundwater flows from an upgradient zone across a control well (W8), three injection wells, and then passes through the downgradient zone installed with seven monitoring wells (W1-W7) (see Fig. S1in the supplemental material). With a high hydraulic conductivity (1.3-3.8 × 10^{-2} cm/sec) and a mean hydraulic gradient of 0.03, the groundwater took 10 hours to flow through the test plot. The groundwater flow pattern was

characterized by injecting a potassium bromide solution (450 mg/L, 3,400 L) into the three injection wells over a 1.5h period two months prior to the test. Peak bromide concentrations were then mapped as an indicator of hydraulic connection among the wells (see Fig. S1 in the supplemental material) (7). The contaminated zone is an unlined aquifer ~8.0 m below ground (bg). The water table, which varies with rain fall events, is ~4 m bg. Overlying the bedrock are (a) an intact weathered shale saprolite, 6−8 m bg, that has unconsolidated characteristics that retain much of the bedding and fracture structure of the parent rock, and (b) a zone of fill with a mixture of disturbed saprolite and gravel, 0−6.0 m bg.

EVO amendment and sampling. EVO was injected into the unconsolidated zone (gravelly fill above the intact saprolite). The composition of EVO (SRS^{TM}, Terra Systems, Wilmington, DE) was 60% (w/w) vegetable oil, 0.3% yeast extract, 0.05% $(NH_4)_3PO_4$, 6% food grade surfactants (mainly arachidic acid), and reminder was water. An EVO emulsion (680 L SRS^{TM} diluted to 3,400 L with site groundwater) was evenly injected into three injection wells over a 2-h time period on February 9, 2009. EVO was injected into the unconsolidated zone (gravel fill above the intact saprolite; beneath the water table) using pumps. After injection, groundwater samples were collected from W1-W8 before injection and 4, 17, 31, 80, 140, and 269 days after the injection by pumping. Before sampling, the wells were purged by pumping ~ 3 times the well volume of groundwater into the well to wash out accumulated dead water in the wells. For microbial community analysis, groundwater was filtered on site with sterile 8-μm filters to remove large particles, followed by filtering with 0.2-μm filters to collect biomass. The filters were immediately frozen, shipped on dry ice to the laboratory, and stored at -80 ºC until DNA extraction.

Groundwater geochemical analysis. Groundwater samples for metal analysis (10 mL) were filtered via 0.3 μm filter and acidified with 0.05 ml of concentrated nitric acids, and then stored at 4ºC until analysis. The source and quality of other chemicals used and analytical methods are described in detail previously (17, 18). U(VI) was measured using a kinetic phosphorescence KPA-11analyzer for U analysis (Chemchek Instruments, Richland,WA). The speciation of U in sediments was determined by XANES and EXAFS as described previously (10). Anions (acetate, NO_3^-, Cl^-, and SO_4^{2-}) were analyzed with an ion chromatograph equipped with an IonPac AS-14 analytical column and an AG-14 guard column (Dionex DX-120, Sunnyvale, CA). Cations (Al, Ca, Fe, Mn, Mg, U, K, etc) were determined using an inductively coupled plasma mass spectrometer (ICPMS) (Perkin Elmer ELAN 6100). Aqueous Fe(II), total Fe, sulfide and COD were measured colorimetrically using a HACH DR 2000 spectrophotometer (Hach Chemical, Loveland, CO). Methane was measured by a TCD gas chromatograph as described by Spalding and Watson (2006, 2008). The EVO or oil concentration in groundwater was indirectly analyzed using volatile sold (VS), which was determined by weight loss on ignition for 1 hour at 550^oC (4). The pH, dissolved oxygen (DO), conductivity, temperature, HCO_3^-, sulfide and Fe(II) of groundwater samples were determined in the wells or immediately in an on-site trailer laboratory at the Oak Ridge site.

GeoChip analysis. Groundwater DNA was extracted from the filters by a freeze-grinding mechanical lysis method (20). DNA quality was assessed by absorbance ratios (260/280 and 260/230 nm) using a NanoDrop ND-1000 Spectrophotometer (NanoDrop Technologies Inc., Wilmington, DE). The final DNA concentrations were quantified by the PicoGreen method (1) using a FLUOstar Optima (BMG Labtech, Jena, Germany) with a Quant-It PicoGreen kit (Invitrogen, Carlsbad, CA).

A comprehensive functional gene array, GeoChip 3.0 was used to analyze the functional composition, structure and dynamics of all 56 microbial communities. GeoChip 3.0 contains > 28,000 probes covering approximately 57,000 gene variants from 292 functional gene families involved in carbon (C), nitrogen (N), phosphorus (P) and sulfur (S) cycling, energy metabolism, antibiotic resistance, metal resistance and organic contaminant degradation. It also has other distinct features, such as a common oligonucleotide as the universal standard for data normalization and comparison (12).

DNA amplification and labeling. In order to produce consistent hybridizations from all samples, a whole community genome amplification was used with 20 ng DNA as the template using the TempliPhi Kit (GE Healthcare, Piscataway, NJ) following the manufacturer's instructions (16). Also, single-strand binding protein (267 ng μL-1) and spermidine (0.1 mM) were added to the reaction mix to improve the amplification efficiency. The reactions were incubated at 30°C for 4 hours and stopped by heating the mixtures at 65°C for 10 min. After amplification, the generated DNA (~3.0 μg) was labeled with the fluorescent dye Cy-5 using random priming method as follows. First, the amplified products were mixed with 20 μL random primers, denatured at 99.9 °C for 5 min, and then immediately chilled on ice. Following denaturation, a labeling master mix containing 2.5 μL dNTP (5 mM dAGC-TP, 2.5 mM dTTP), 1 μL Cy-5 dUTP (Amersham, Piscataway, NJ), 80 U of the large Klenow fragment (Invitrogen, Carlsbad, CA), and 2.5 μL water was added, incubated at 37 °C for 5 hours, and heated at 95°Cfor 3 min. Labeled DNA was purified using QIA quick purification kit (Qiagen, Valencia, CA) according to the manufacturer's instructions, measured on a NanoDrop ND-1000 spectrophotometer (NanoDrop Technologies Inc., Wilmington, DE), and then dried down in a SpeedVac (ThermoSavant, Milford, MA) at 45°C for 45 min.

GeoChip hybridization and image analysis. The labeled DNA was re-suspended in 56 µl hybridization solution containing 45% formamide, 3 × SSC, 10.0 µg of unlabeled herring sperm DNA (Promega, Madison, WI), and 0.1% SDS, and the mix was denatured at 95°C for 5 min and kept at 50°C until it was deposited directly onto a microarray. Hybridizations were performed on a MAUI Hybridization System (BioMicro Systems, Salt Lake City, UT) at 42°C for 12 h with mixing. After washing and drying, the microarray was scanned by a ScanArray Express Microarray Scanner (Perkin Elmer, Boston, MA) at 633 nm using a laser power of 90% and a photomultiplier tube (PMT) gain of 75%. The ImaGene version 6.0 (Biodiscovery, El Segundo, CA) was then used to determine the intensity of each spot, and identify poor-quality spots.

Raw data from ImaGene were submitted to Microarray Data Manager in our website (http://ieg.ou.edu/microarray/) and analyzed using the data analysis pipeline with the following major steps: (i) The spots flagged as 1 or 3 by Imagene and with a signal to noise ratio (SNR) less than 2.0 (9) were removed as poor-quality spots; (ii) After removing the bad spots, normalized intensity of each spot was calculated by dividing the signal intensity of each spot by the mean intensity of the microarray; (iii) If any of replicates had (signal–mean) more than two times the standard deviation, this replicate was moved as an outlier. This process continued until no such replicates were identified; (iv) At least 0.34 time of the final positive spots (probes), or a minimum of two spots was required for each gene; and (v) If a probe appeared in one sample among the total of 7 samples for each time point, it was removed for data reliability .

Statistical analysis. Preprocessed GeoChip data and geochemical data were further analyzed using various statistical methods as described elsewhere (8, 11, 13, 15, 19).

Hierarchical clustering analysis. Hierarchical clustering for microbial community structure and composition was performed with CLUSTER 3.0 using uncentered correlations and the

complete average linkage for both genes and samples, and trees were visualized in TREEVIEW (6). The effects of EVO amendment on relative abundance of various functional genes were analyzed by standard t-test. The relative abundance was calculated by dividing the total signal intensity of detected individual gene sequences for each gene or gene group by the total signal intensity of all genes detected on the GeoChip.

Multivariate and direct gradient analysis. In this study, three different non-parametric analyses for multivariate data were used to examine whether EVO amendment has significant effects on groundwater microbial communities: analysis of similarities (ANOSIM) (5), non-parametric multivariate analysis of variance (Adonis) using distance matrices (2), and multi-response permutation procedure (MRPP). We used Jaccard (non-quantitate) and Bray-Curtis (quantitate) similarity indexes to calculate distance matrix for ANOSIM, Adonis and MRPP analyses. All three methods are based on dissimilarities among samples and their rank order in different ways to calculate test statistics, and the Monte Carlo permutation is used to test the significance of statistics.

Mantel test. To elucidate the inter-relationships between groundwater geochemical variables and the abundance of functional genes of microbial community detected by GeoChip, the Mantel test was employed. Mantel test is an appropriate statistic method to measure the correlation between dissimilarity matrices and the significance of the statistics evaluated by permuting the matrixes (3). The geochemical data were standardized to zero mean and unit deviation before calculation. The Bray-Curtis distance was used to construct the dissimilarity matrixes of communities and environmental variables respectively. All the analyses were performed by the vegan package in R (R Development Core Team, 2011).

B. Supplemental Figures

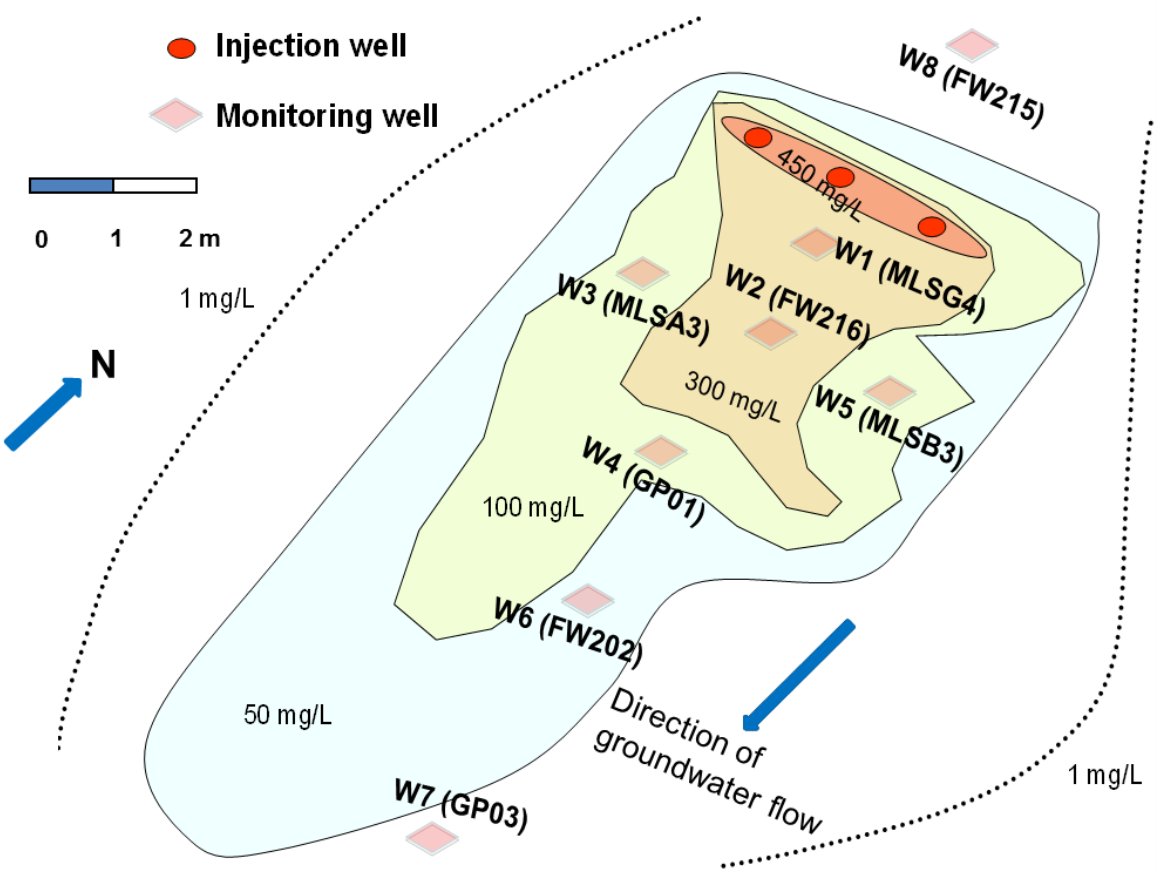

FIG S1 The well system for *in situ* bioremediation of U(VI) with EVO amendment, showing groundwater flow direction and distribution of a upgradient control well, W8 (FW215) and seven downgradient monitoring wells, W1 (MLSG4), W2 (FW216-1), W3 (MLSA8), W4 (GP01), W5 (MLSB3), W6 (FW202-2), and W7 (GP03). The peak bromide concentration distribution was drawn based on data from a previous tracer test with injection of bromide solution (450 mg/L) into the three injection wells as an indicator of hydraulic connection among the wells.

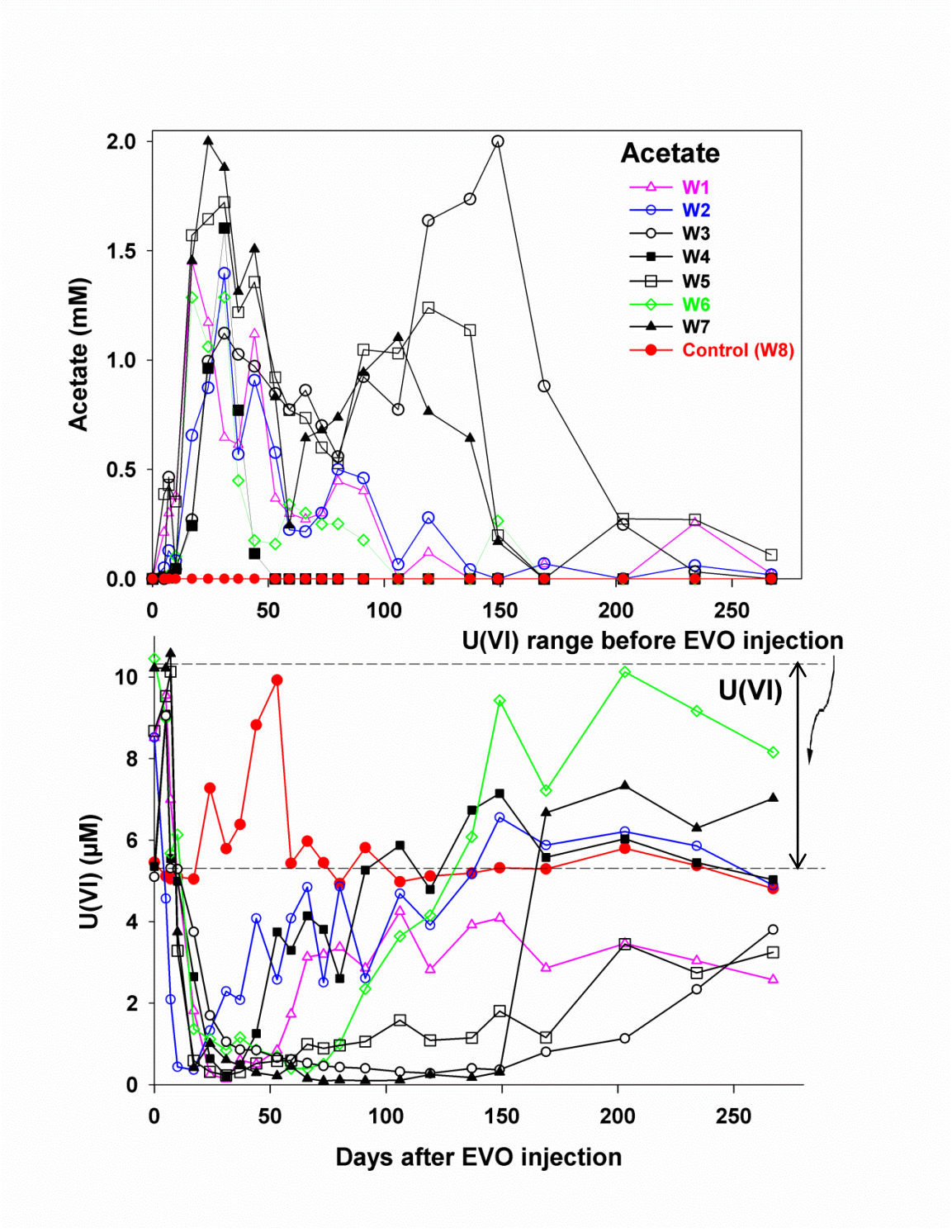

173

174

175

176

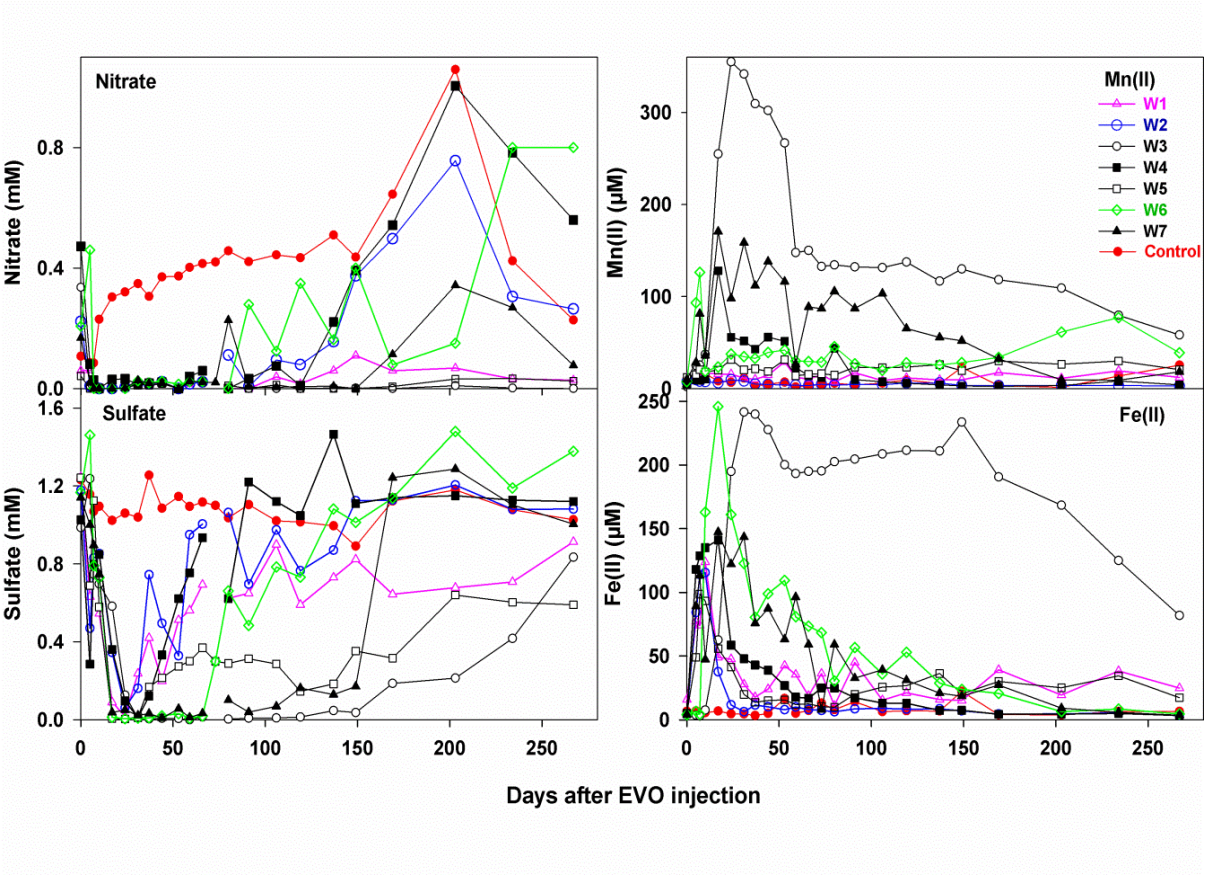

177

178 **FIG S2** Changes in groundwater concentrations of acetate, U(VI), nitrate, sulfate, Mn(II), and

179 Fe(II) in the eight monitoring wells (W1-W8) after EVO amendment. The U(VI) concentration

180 range before EVO injection is shown.

181

182

183

184

185

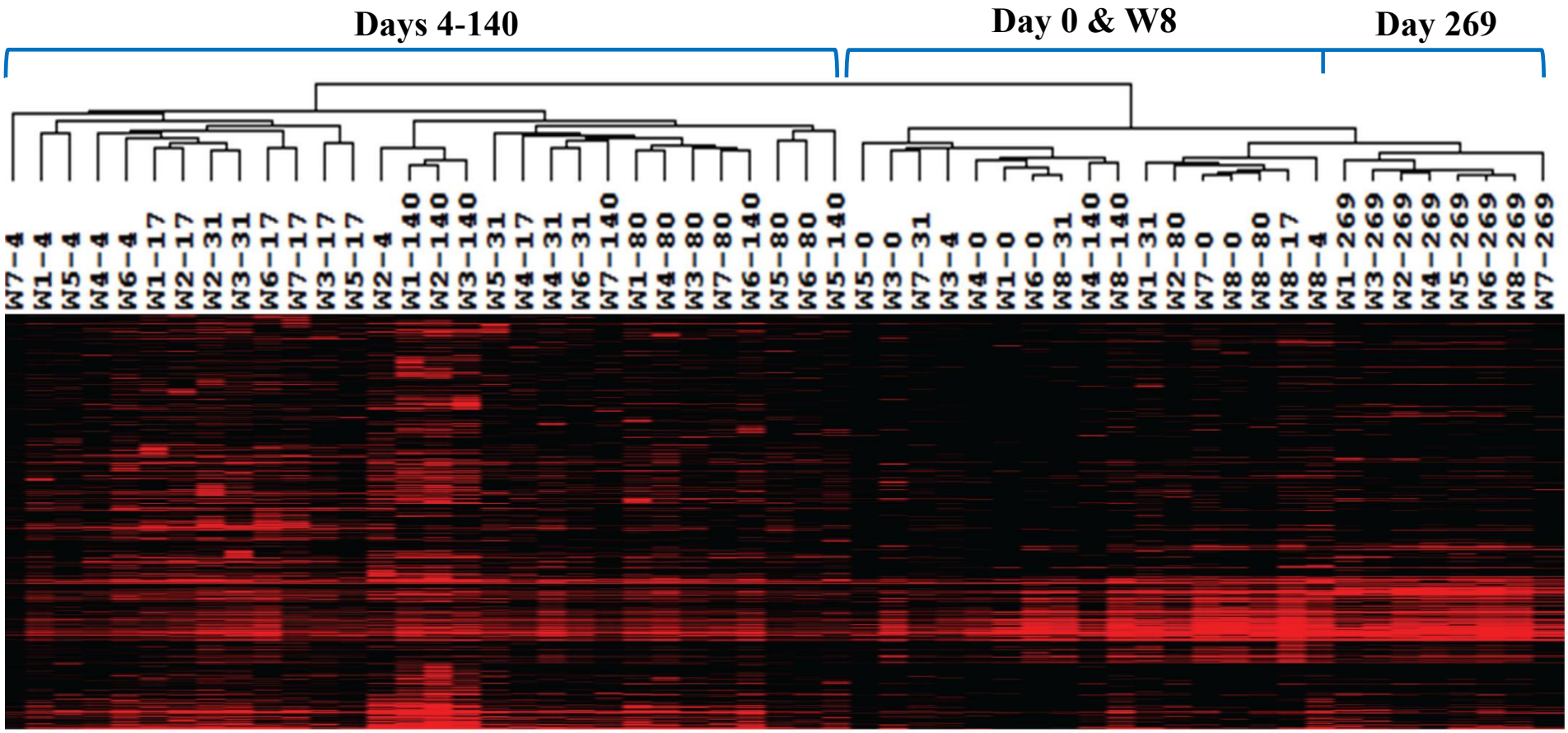

196

197 **FIG S3** Hierarchical cluster analysis of all functional genes detected in at least two out of the seven downgradient wells (W1-W7) at
198 each time point (0, 4, 17, 31, 80, 140, and 269 days). Genes detected in an upgradient control well (W8) at these time points were also
199 included. In the sample IDs, the number following dash represents days after EVO amendment, with 0 = before EVO amendment.
200 Results were generated in Cluster3.0 and visualized using TreeView. Black indicates signal intensities below background, while red
201 indicates signal intensities above background and brighter red indicates higher signal intensities. This method about heatmap
202 preparation and explanation also applies to supplemental material Figs S5, S7, S8, S11, and S12.

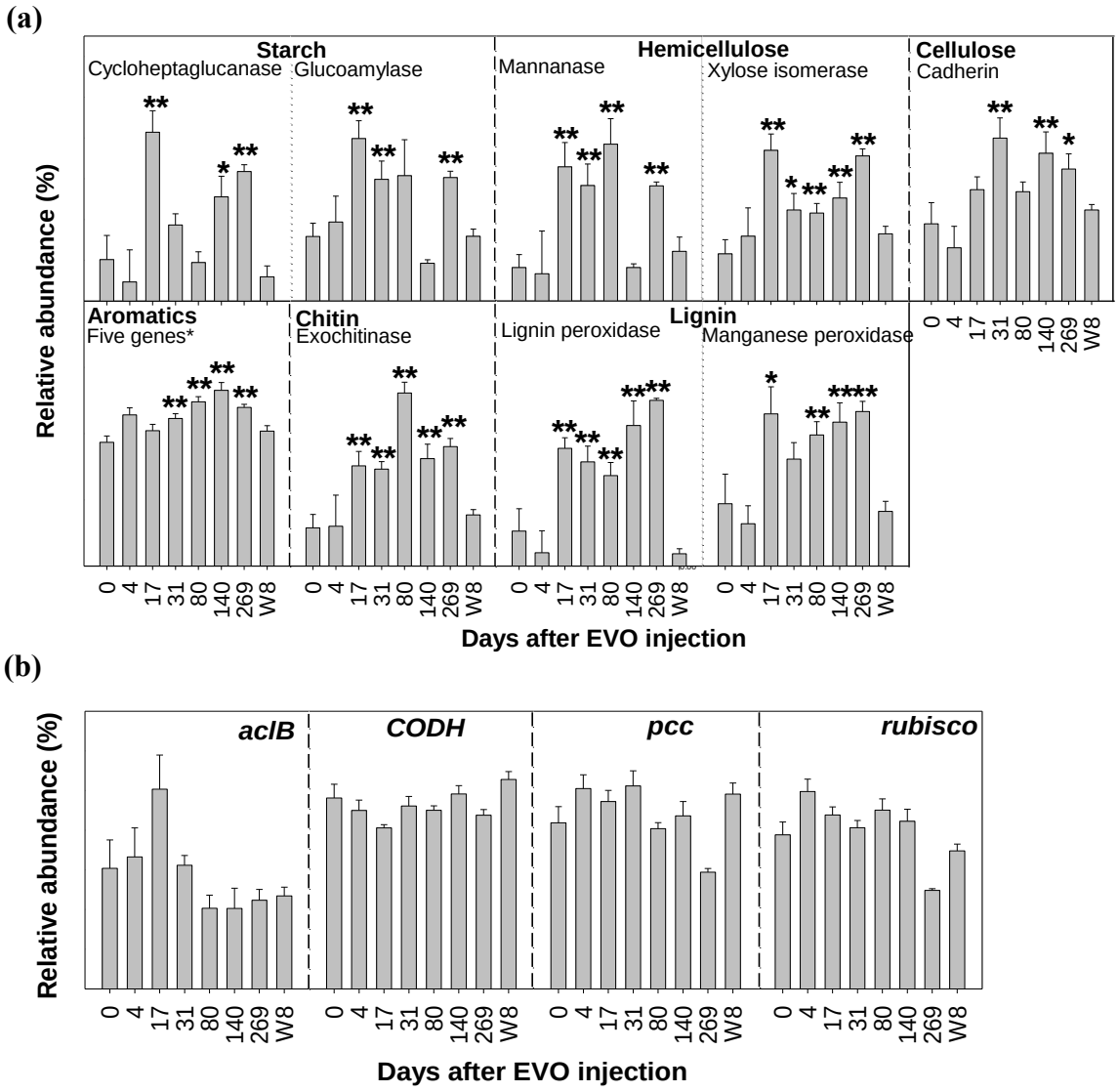

FIG S4 Average relative abundance of (a) representative genes involved in the degradation of organic carbon compounds and (b) genes for CO_2 fixation in seven downgradient wells (W1-W7) after EVO amendment. Because the abundance varies for each gene depending on probes on the array, y axis scales for gene abundance are not shown. The significance (**P <0.05, *<0.10) was tested between each time point and 0d using the Student's t-test. Data detected at the same time points in a upgradient control well (W8) were also included for comparison. All data are presented as mean ± SE of measurements in the seven downgradient wells (W1-W7) at each time point, and mean ± SE of seven measurements in W8 over time. The relative abundance was

calculated by dividing the total signal intensity of detected individual gene sequences for each gene or gene group by the total signal intensity of all genes detected on the GeoChip. The carbon substrates of these genes are presented in order from labile to recalcitrant. The five stimulated genes for aromatic degradation included isocitrate lyase, malate synthase, limonene-1,2-epoxide hydrolase, limonene monooxygenase, and vanillin dehydrogenase. *aclB*: ATP citrate lyase; *CODH*: carbon monoxide dehydrogenase; *pcc*: propionyl-CoA carboxylase; *rubisco*: ribulose-l,5-bisphosphate carboxylase/oxygenase.

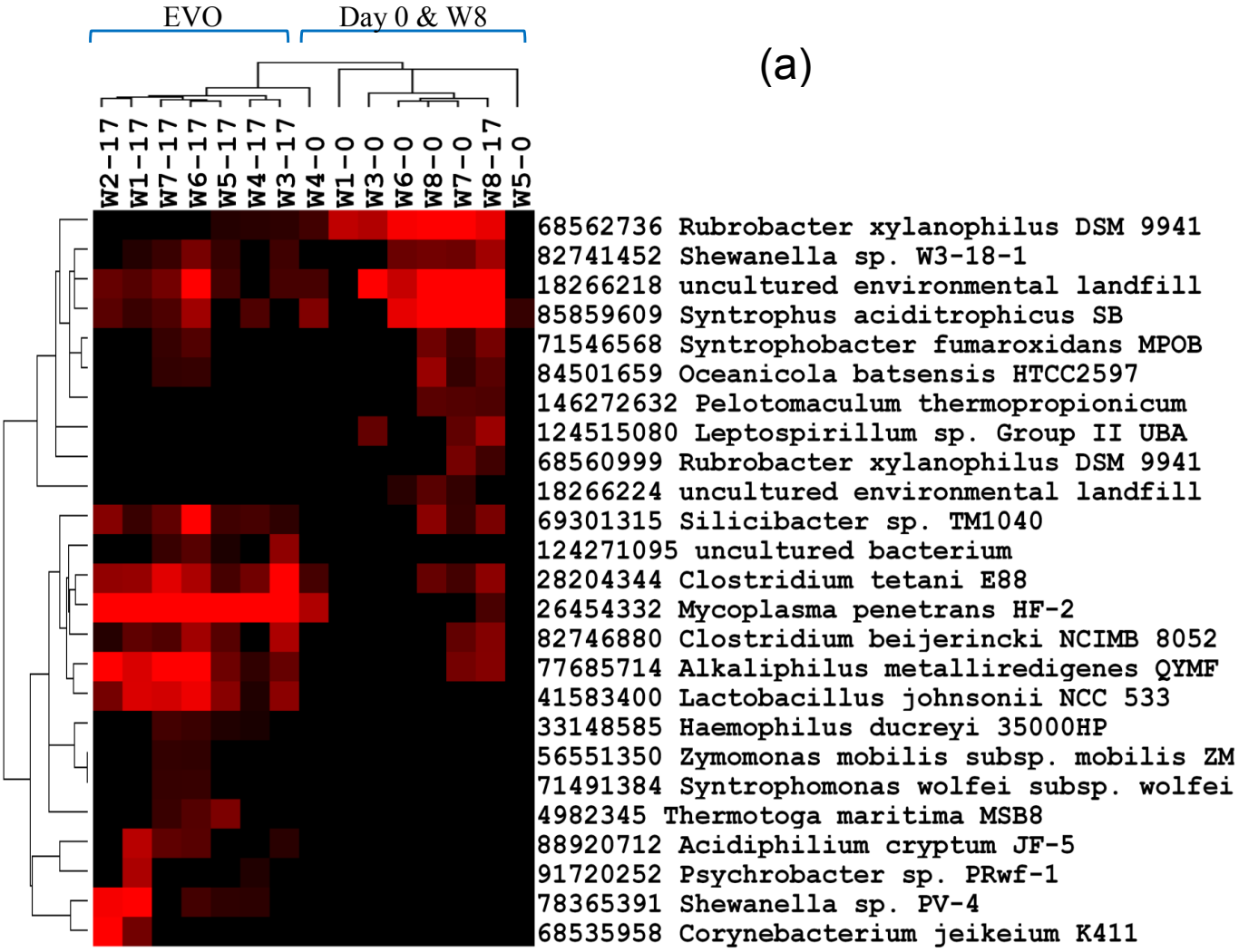

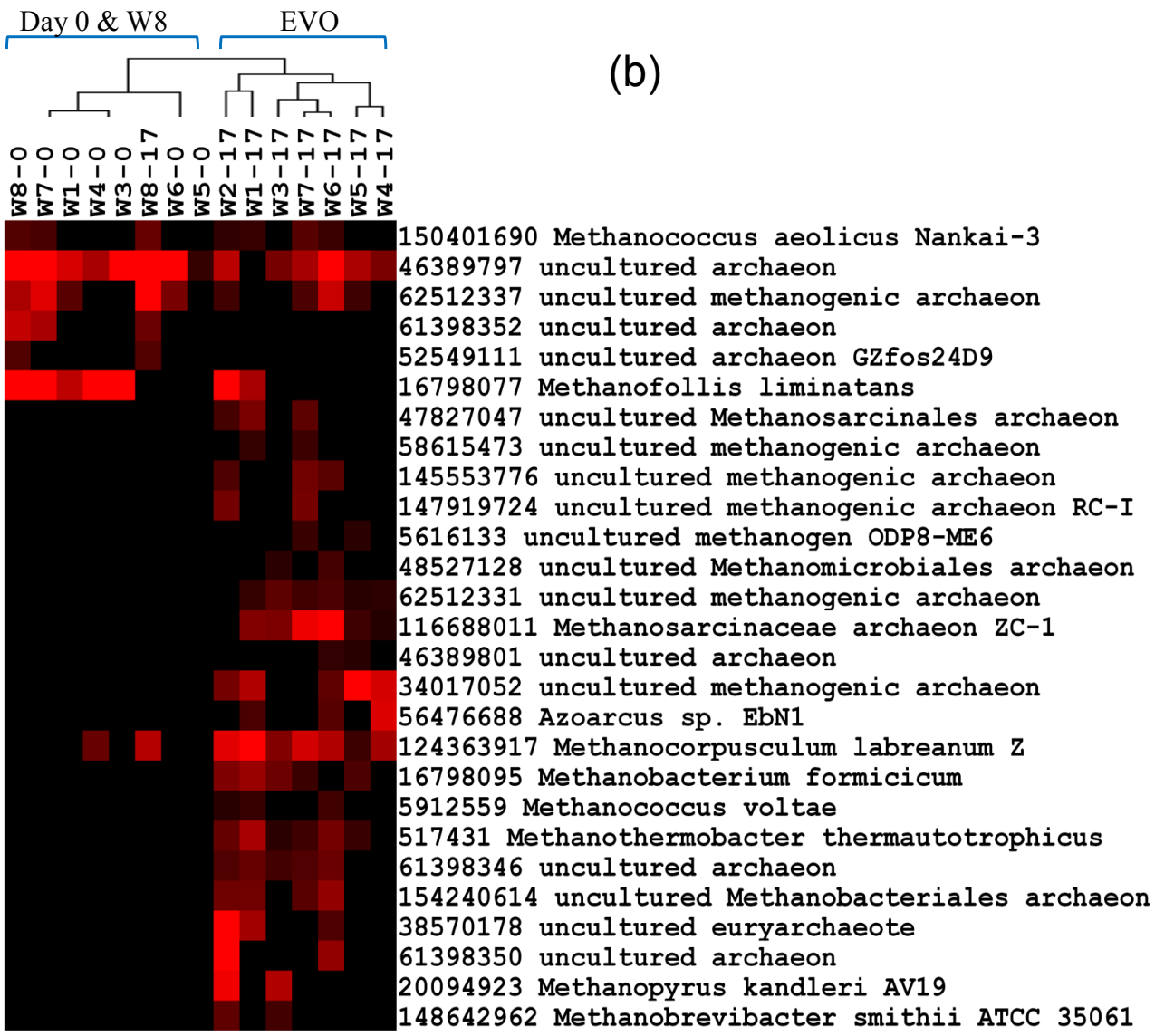
Day 0 & W8
EVO
(b)
W8−0
W7−0
W1−0
W4−0
W3−0
W8−17
W6−0
W5−0
W2−17
W1−17
W3−17
W7−17
W6−17
W5−17
W4−17
150401690 Methanococcus aeolicus Nankai-3
46389797 uncultured archaeon
62512337 uncultured methanogenic archaeon
61398352 uncultured archaeon
52549111 uncultured archaeon GZfos24D9
16798077 Methanofollis liminatans
47827047 uncultured Methanosarcinales archaeon
58615473 uncultured methanogenic archaeon
145553776 uncultured methanogenic archaeon
147919724 uncultured methanogenic archaeon RC-I
5616133 uncultured methanogen ODP8-ME6
48527128 uncultured Methanomicrobiales archaeon
62512331 uncultured methanogenic archaeon
116688011 Methanosarcinaceae archaeon ZC-1
46389801 uncultured archaeon
34017052 uncultured methanogenic archaeon
56476688 Azoarcus sp. EbN1
124363917 Methanocorpusculum labreanum Z
16798095 Methanobacterium formicicum
5912559 Methanococcus voltae
517431 Methanothermobacter thermautotrophicus
61398346 uncultured archaeon
154240614 uncultured Methanobacteriales archaeon
38570178 uncultured euryarchaeote
61398350 uncultured archaeon
20094923 Methanopyrus kandleri AV19
148642962 Methanobrevibacter smithii ATCC 35061

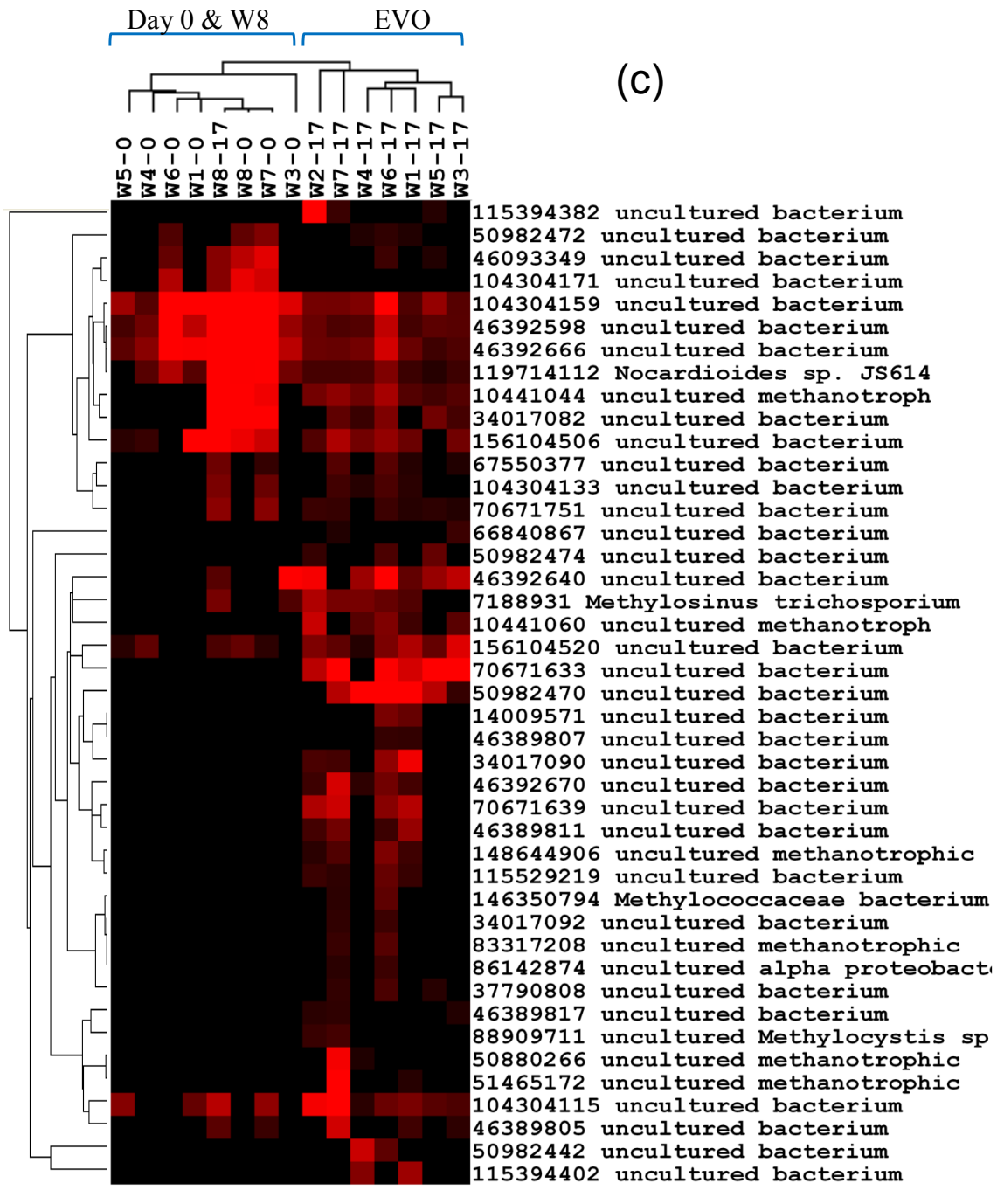

FIG S5 Enrichment of key genes involved in (a) acetongenesis (*fhs*), (b) methanogenesis (*mcrA*), and (c) methane oxidation (*pmoA*) in the seven downgradient wells (W1-W7) 17 days after EVO amendment. In the sample ID, the number following dash is 0 for Day 0 samples, and is 17 for Day 17 samples. Genes detected in the control well (W8) at these time points were also included. The protein id numbers and derived microorganisms are shown.

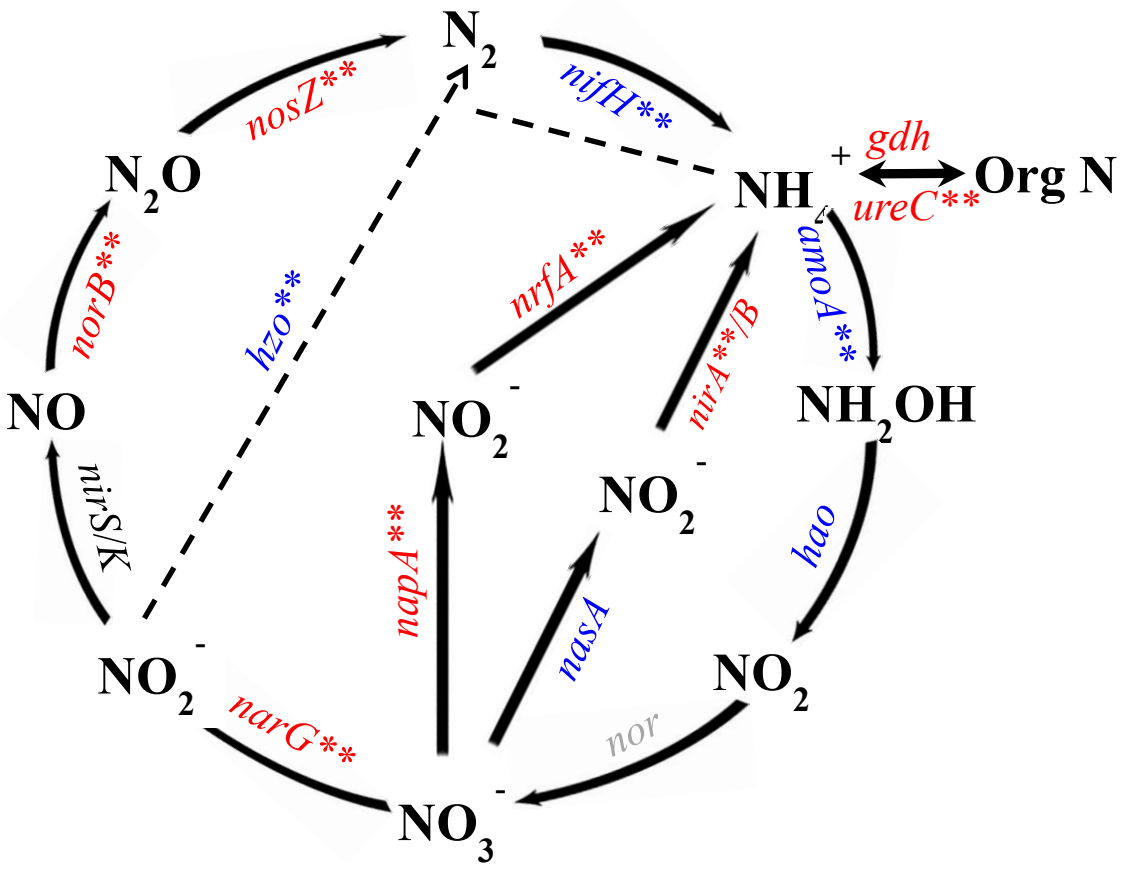

FIG S6 Changes in the relative abundance of genes involved in N cycling in the seven downgradient wells (W1-W7) after EVO amendment. For each functional gene, colors mean that this gene had a higher (red), lower (blue), or similar (black) relative abundance than that before EVO amendment. Gray-colored genes were not targeted by this GeoChip. All data are mean of seven wells. The Student's t-tests were performed to determine the significance of the changes (**P<0.05) and genes showed changes at ≥two out of the six time points were counted. The relative abundance was calculated by dividing the total signal intensity of detected individual gene sequences for each gene by the total signal intensity of all genes detected on the GeoChip. More detailed temporal dynamics of these genes are shown in Fig 2. Description of the genes: (a) *narG* encoding nitrate reductase, *nirS* and *nirK* encoding nitrite reductase, *norB* encoding nitric oxide reductase, *nosZ* encoding nitrous oxide reductase, responsible for denitrification; (b) *napA*

encoding nitrate reductase, *nrfA* encoding c-type cytochrome nitrite reductase, responsible for dissimilatory nitrate reduction; (c) *nasA* encoding nitrate reductase, *nir* encoding nitrite reductase, responsible for assimilatory nitrate reduction; (d) *hzo* encoding hydrazine oxidoreductase responsible for anammox; (e) *nifH* encoding nitrogenase responsible for N_2 fixation; (f) *amoA* encoding ammonia monooxygenase, *hao* encoding hydroxylamine oxidoreductase, responsible for nitrification; (g) *gdh* encoding glutamate dehydrogenase, *ureC* encoding urease, responsible for ammonification.

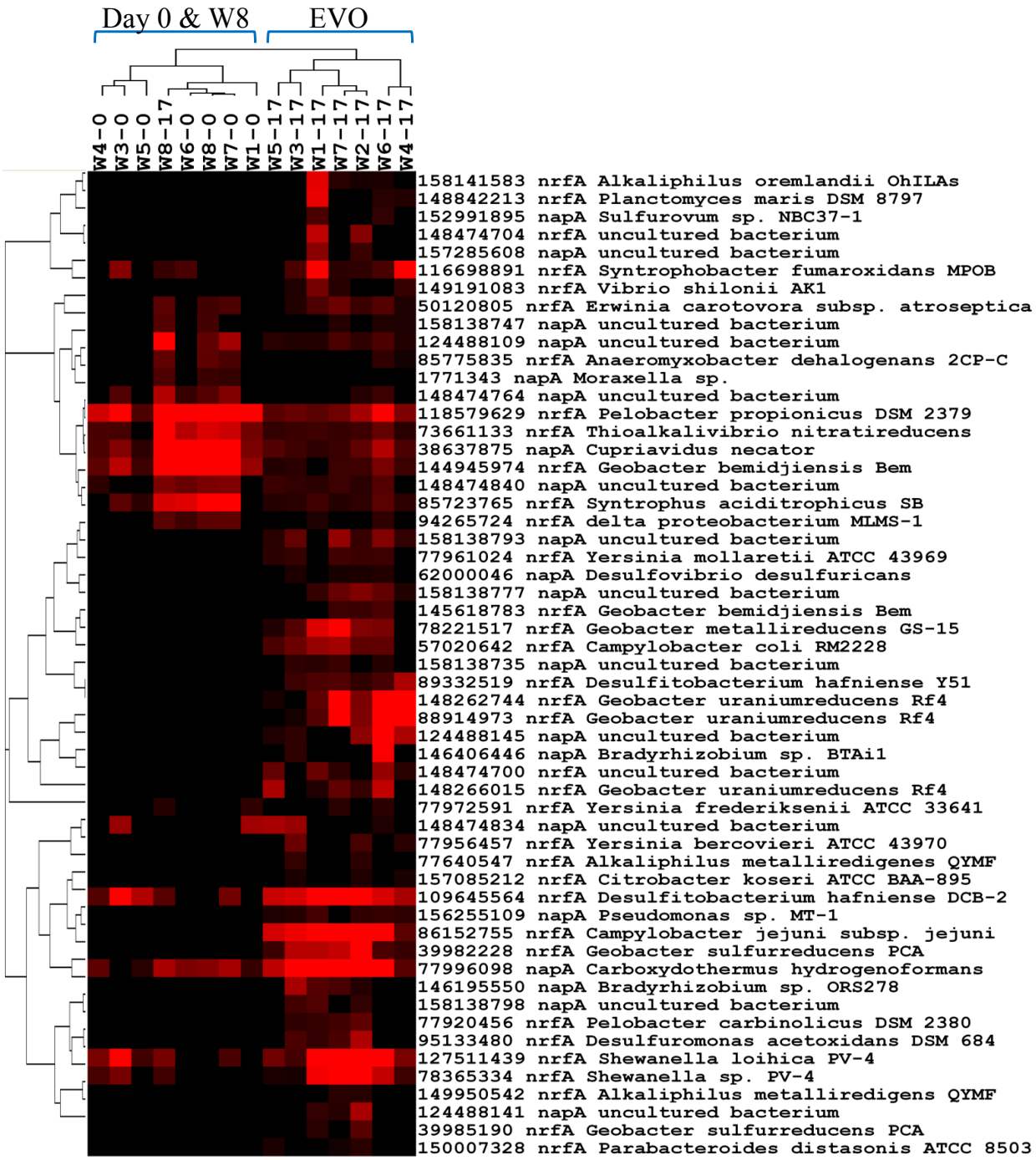

FIG S7 Enrichment of key genes (*napA* encoding nitrate reductase and *nrfA* encoding c-type cytochrome nitrite reductase) involved in dissimilatory nitrate reduction in the seven downgradient wells (W1-W7) 17 days after EVO amendment. In the sample ID, the number following dash is 0 for Day 0 samples, and is 17 for Day 17 samples. Genes detected in the control well (W8) at these time points were also included. The protein id numbers and derived microorganisms are shown.

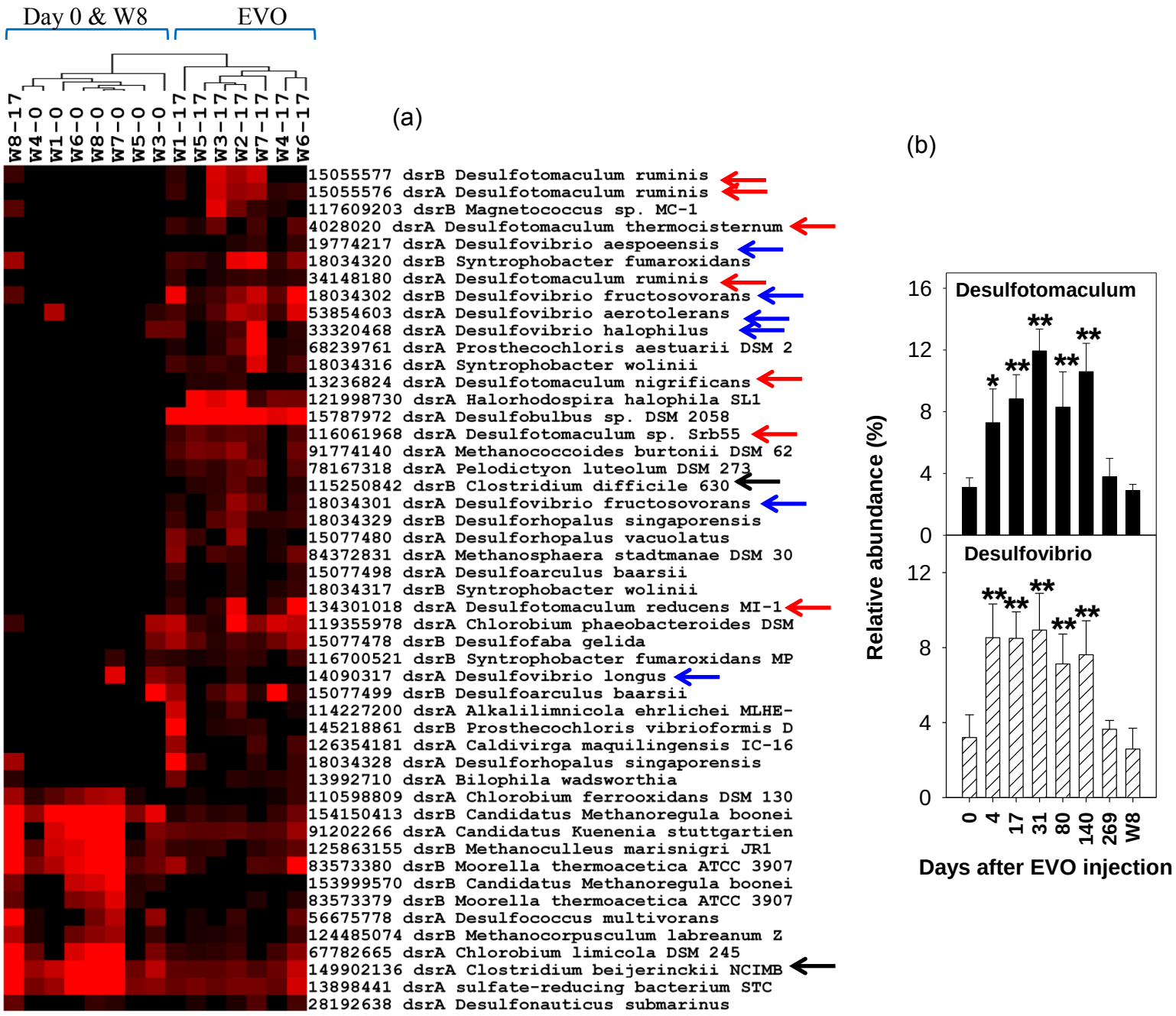

380 **FIG S8** Enrichment of *dsrAB* genes encoding dissimilatory sulfite reductase: (a) two distinct
381 major clusters showing *dsrAB* genes from known SRB enriched in the seven downgradient wells
382 (W1-W7) 17 days after EVO amendment. In the sample ID, the number following dash is 0 for
383 Day 0 samples, and is 17 for Day 17 samples. Data detected in the control well (W8) at these
384 time points were also included. The protein id numbers and derived SRB are shown. Arrows in
385 red indicate genes from *Desulfotomaculum*, in blue indicate genes from *Desulfovibrio*, and black
386 arrows indicate genes from *Clostridium*. (b) changes in average relative abundance of *dsrAB*

genes from two genera in in the seven downgradient wells after EVO amendment. The significance (**P <0.05, *<0.10) was tested between each time point and 0d using the Student's t-test. All data are presented as mean ± SE of measurements in the seven downgradient wells (W1-W7) at each time point, and mean ± SE of seven measurements in W8 over time.

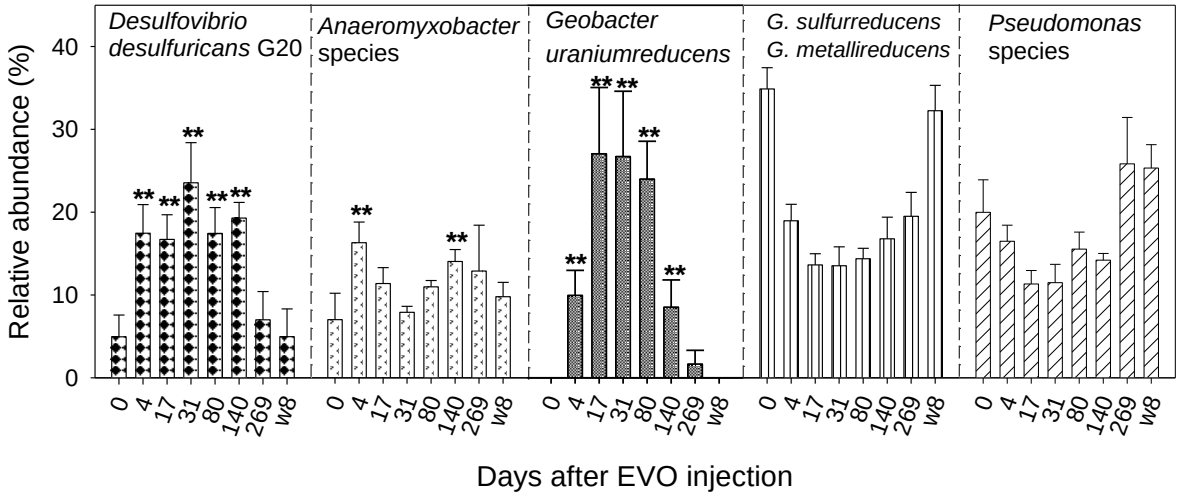

FIG S9 Changes in the average relative abundance of major cytochrome-containing populations in the seven downgradient wells after EVO amendment. The significance (**P <0.05, *<0.10) was tested between each time point and 0d using the Student's t-test. Data detected at the same time points in a upgradient control well (W8) were also included for comparison. All data are presented as mean ± SE of measurements in the seven downgradient wells (W1-W7) at each time point, and mean ± SE of seven measurements in W8 over time. The mean signal intensity was calculated by dividing the total signal intensity of all genes detected in a species by the number of genes from this species, and the relative abundance was calculated by dividing the mean signal intensity by the total signal intensity of all cytochrome genes detected. *Anaeromyxobacter* spp. include *A. dehalogenans* 2CP-C and *A.* sp. Fw109-5. *Pseudomonas* spp. primarily include *P. putida* KT2440, *P. stutzeri* A1501, *P. syringae, P. fluorescens,* and *P. aeruginosa* PA7.

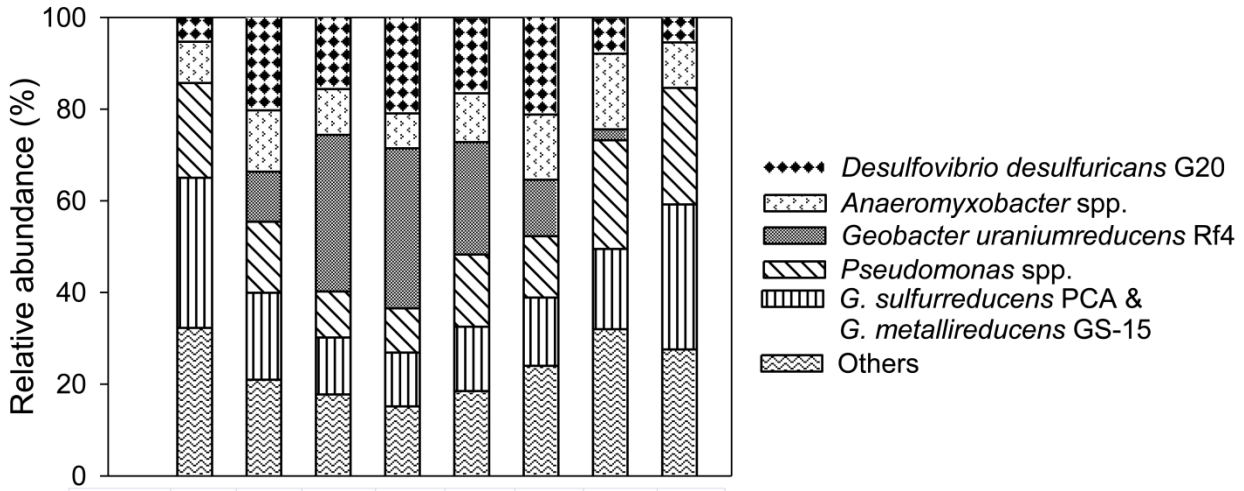

	0d	4d	17d	31d	80d	140d	269d	W8
Gene#	11	28	42	31	32	42	19	17
Shannon	2	3	3.4	3.1	3.2	3.4	2.6	2.4
Simpson	6.6	18.2	21.3	16.8	18.6	20.3	11.2	10.2

FIG S10 Changes in the composition and structure of cytochrome-containing communities in the seven downgradient wells after EVO amendment. Data detected at the same time points in an upgradient control well (W8) were also included for comparison. The table shows total number and Shannon–Weiner (*H'*) and Simpson's (1/*D*) diversity indices of detected cytochrome genes. The mean signal intensity was calculated by dividing the total signal intensity of all genes detected in a species by the number of genes from this species, and the relative abundance was calculated by dividing the mean signal intensity by the total signal intensity of all cytochrome genes detected. All data are presented as mean of measurements in the seven downgradient wells (W1-W7) at each time point and mean of seven measurements in W8 over time. SE and *P* values are shown in the Supplemental material Fig S9. *Anaeromyxobacter* spp. include *A. dehalogenans* 2CP-C and *A.* sp. Fw109-5. *Pseudomonas* spp. primarily include *P. putida* KT2440, *P. stutzeri* A1501, *P. syringae, P. fluorescens,* and *P. aeruginosa* PA7. Others include *Rhodobacter, Haloarcula, Sinorhizobium, Halorubrum,* and *Candida*.

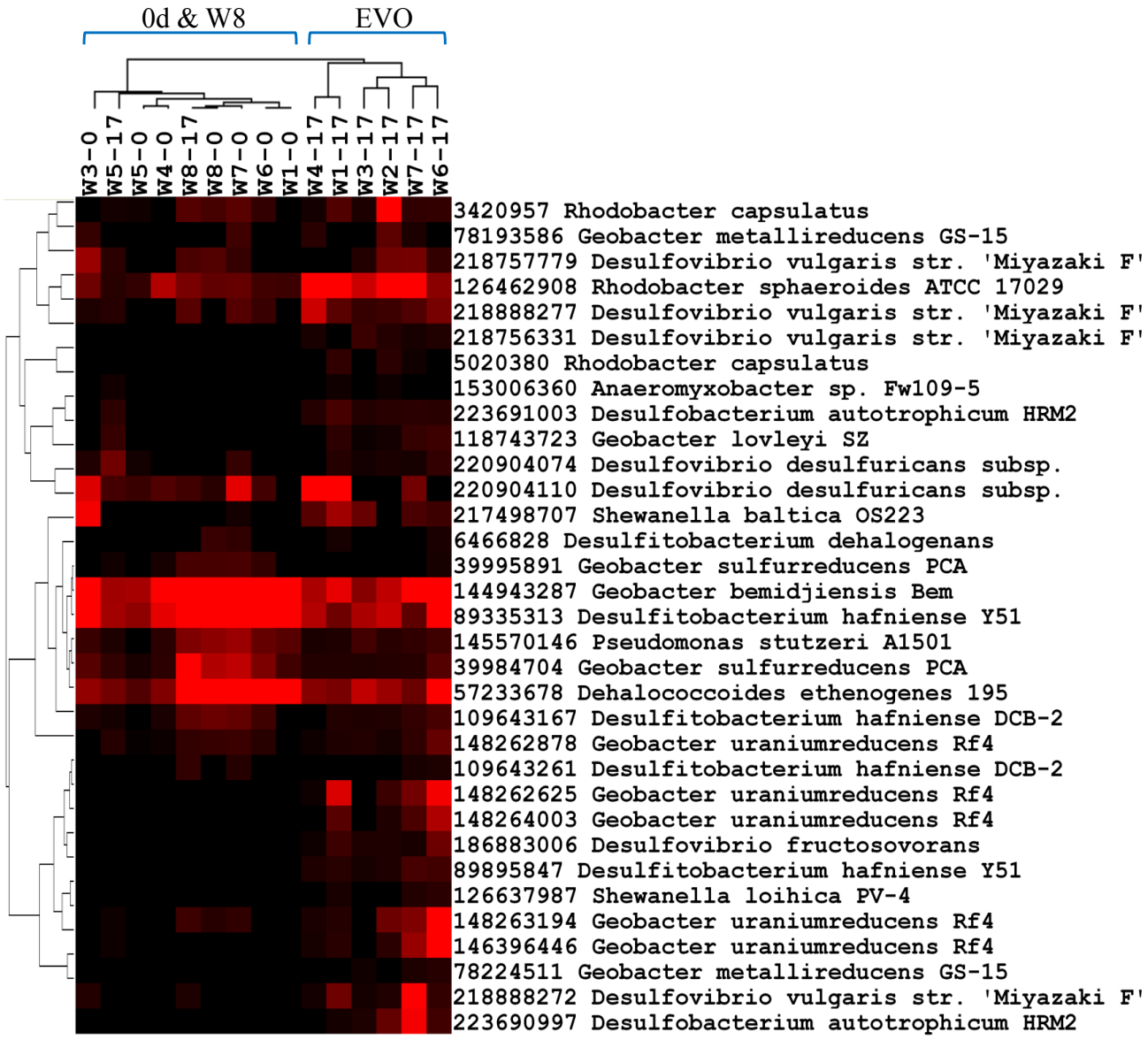

FIG S11 Enrichment of hydrogenase genes in the seven downgradient wells (W1-W7) 17 days after EVO amendment. In the sample ID, the number following dash is 0 for Day 0 samples, and is 17 for Day 17 samples. Data detected in the control well (W8) at these time points were also included. The protein id numbers and derived microorganisms are shown.

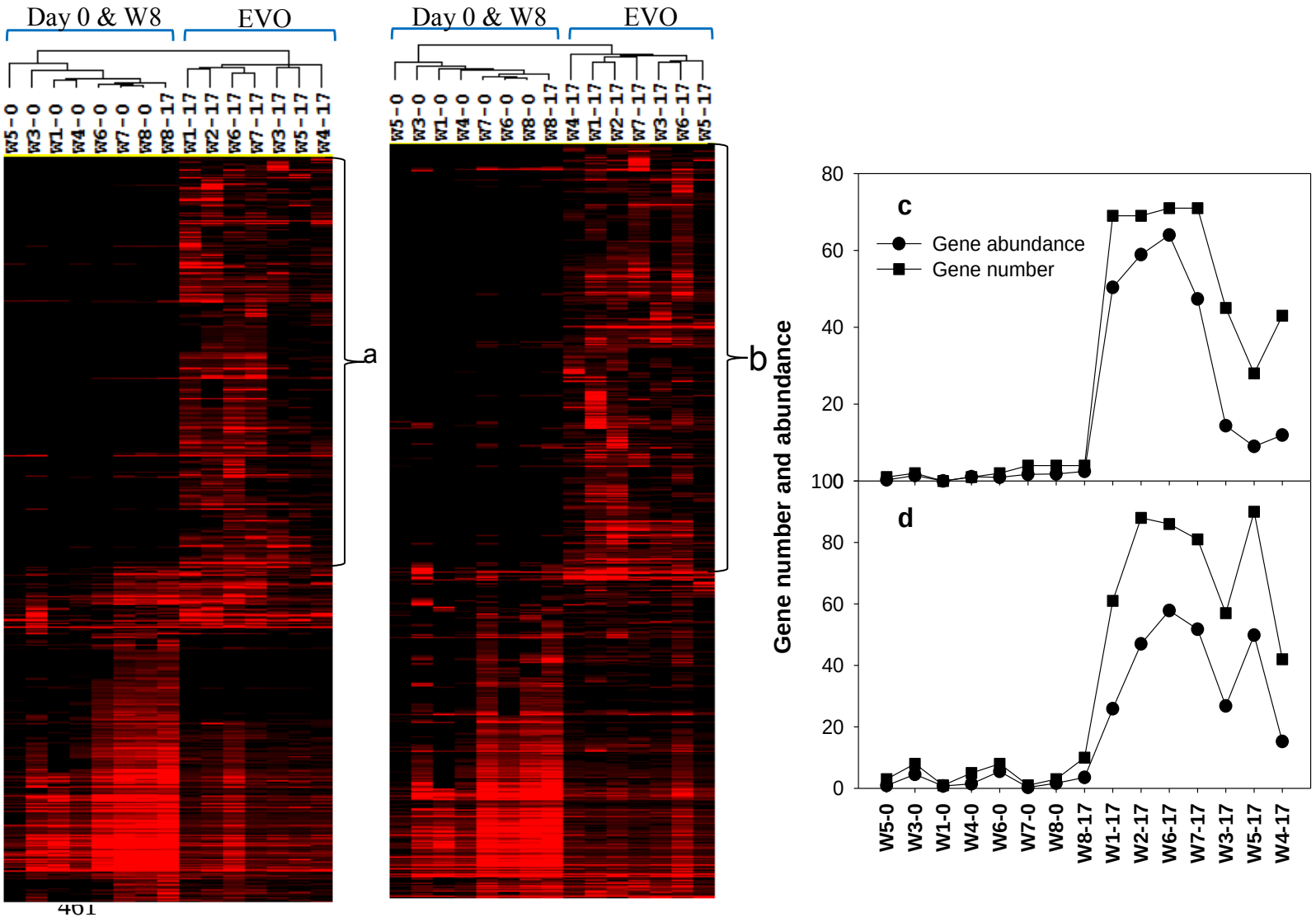

FIG S12 Enrichment of metal resistance (a and c) and organic contaminant degradation (b and d) genes in the seven downgradient wells (W1-W7) at 17 days after EVO amendment. In the sample ID, the number following dash is 0 for Day 0 samples, and is 17 for Day 17 samples. Data detected in the control well (W8) at these time points were also included. Panels a and b show more genes were detected after EVO amendment, and panels c and d show increased ($P <$ 0.001) number and abundance of genes derived from the genera which have species known to be capable of U(VI) reduction. These selected genera included *Geobacter*, *Anaeromyxobacter*, *Desulfovibrio*, *Desulfitobacterium*, *Desulfotomaculum*, *Acidovorax*, *Pseudomonas*, *Salmonella*, *Clostridium*, and *Deinococcus* for metal resistance genes [e.g., efflux transporters for Cr (*ChrA*)

and Zn (*czcA/D* and *zntA*)]. For organic contaminant degradation genes (e.g., *toluene dioxygenase* for trichloroethylene degradation), the selected genera included *Geobacter*, *Desulfovibrio*, *Desulfitobacterium*, *Acidovorax*, *Pseudomonas*, *Clostridium*, and *Deinococcus*.

C. Supplemental Table

TABLE S1 Significance ($P < 0.05$, boldface values) of the effects of EVO amendment on overall functional structure of the groundwater microbial community and concentrations of acetate and five electron acceptors[a] using three statistical tests[b]

Difference from 0d	Microbial community			Geochemical variables[a]		
	MRPP	ANOSIM	Adonis	MRPP	ANOSIM	Adonis
4d	**0.001**	**0.002**	**0.001**	0.138	0.150	0.100
17d	**0.001**	**0.001**	**0.001**	**0.001**	**0.002**	**0.001**
31d	**0.025**	**0.023**	**0.017**	**0.002**	**0.001**	**0.001**
80d	**0.005**	**0.004**	**0.006**	**0.005**	**0.007**	**0.004**
140d	**0.010**	**0.007**	**0.009**	**0.039**	**0.043**	**0.034**
269d	**0.003**	**0.004**	**0.004**	0.058	**0.049**	0.184
4-17d vs. 80-140d[c]	**0.006**	**0.002**	**0.005**	0.192	0.398	0.288

[a]included acetate NO_3^-, Fe(II), Mn(II), U(VI), and SO_4^{-2}.

[b]All three tests are non-parametric multivariate analyses based on dissimilarities between samples in different groups using bray-cutis distance. MRPP, multiple response permutation procedure, a nonparametric procedure that does not depend on assumptions such as normally distributed data or homogeneous variances, but rather depends on the internal variability of the data; ANOSIM, analysis of similarity; Adonis, non-parametric multivariate analysis of variance (MANOVA) with the adonis function. The difference is significant when at least two tests gave P values of < 0.05.

[c]Difference between two groups.

D. Supplemental references

1. **Ahn, S. J., J. Costa, and J. R. Emanuel.** 1996. PicoGreen quantitation of DNA: Effective evaluation of samples pre- or post-PCR. Nucleic Acids Res **24:**2623-2625.
2. **Anderson, M. J.** 2001. A new method for non-parametric multivariate analysis of variance. Austral Ecol **26:**32-46.
3. **Borcard, D., P. Legendre, and P. Drapeau.** 1992. Partialling out the Spatial Component of Ecological Variation. Ecology **73:**1045-1055.
4. **Borden, R. C.** 2007. Effective distribution of emulsified edible oil for enhanced anaerobic bioremediation. J Contam Hydrol **94:**1-12.
5. **Clarke, K. R.** 1993. Nonparametric Multivariate Analyses of Changes in Community Structure. Aust J Ecol **18:**117-143.
6. **de Hoon, M. J. L., S. Imoto, J. Nolan, and S. Miyano.** 2004. Open source clustering software. Bioinformatics **20:**1453-1454.
7. **Gihring, T. M., G. X. Zhang, C. C. Brandt, S. C. Brooks, J. H. Campbell, S. Carroll, C. S. Criddle, S. J. Green, P. Jardine, J. E. Kostka, K. Lowe, T. L. Mehlhorn, W. Overholt, D. B. Watson, Z. M. Yang, W. M. Wu, and C. W. Schadt.** 2011. A Limited Microbial Consortium Is Responsible for Extended Bioreduction of Uranium in a Contaminated Aquifer. Appl Environ Microb **77:**5955-5965.
8. **He, Z. L., M. Y. Xu, Y. Deng, S. H. Kang, L. Kellogg, L. Y. Wu, J. D. Van Nostrand, S. E. Hobbie, P. B. Reich, and J. Z. Zhou.** 2010. Metagenomic analysis reveals a marked divergence in the structure of belowground microbial communities at elevated CO2. Ecol Lett **13:**564-575.

9. **He, Z. L., and J. Z. Zhou.** 2008. Empirical evaluation of a new method for calculating signal-to-noise ratio for microarray data analysis. Appl Environ Microb **74:**2957-2966.
10. **Kelly, S. D., K. M. Kemner, J. Carley, C. Criddle, P. M. Jardine, T. L. Marsh, D. Phillips, D. Watson, and W. M. Wu.** 2008. Speciation of uranium in sediments before and after in situ biostimulation. Environ Sci Technol **42:**1558-1564.
11. **Liang, Y., Z. He, L. Wu, Y. Deng, G. Li, and J. Zhou.** 2010. Development of a common oligonucleotide reference standard for microarray data normalization and comparison across different microbial communities. Appl Environ Microb **76:**1088-1094.
12. **Liang, Y. T., Z. L. He, L. Y. Wu, Y. Deng, G. H. Li, and J. Z. Zhou.** 2010. Development of a Common Oligonucleotide Reference Standard for Microarray Data Normalization and Comparison across Different Microbial Communities. Appl Environ Microb **76:**1088-1094.
13. **Lu, Z., Y. Deng, J. D. Van Nostrand, Z. He, J. Voordeckers, A. Zhou, Y. J. Lee, O. U. Mason, E. A. Dubinsky, K. L. Chavarria, L. M. Tom, J. L. Fortney, R. Lamendella, J. K. Jansson, P. D'Haeseleer, T. C. Hazen, and J. Zhou.** 2011. Microbial gene functions enriched in the Deepwater Horizon deep-sea oil plume. The ISME journal.
14. **Moon, J. W., Y. Roh, T. J. Phelps, D. H. Phillips, D. B. Watson, Y. J. Kim, and S. C. Brooks.** 2006. Physicochemical and mineralogical characterization of soil-saprolite cores from a field research site, Tennessee. J Environ Qual **35:**1731-1741.
15. **Van Nostrand, J. D., L. Wu, W. M. Wu, Z. Huang, T. J. Gentry, Y. Deng, J. Carley, S. Carroll, Z. He, B. Gu, J. Luo, C. S. Criddle, D. B. Watson, P. M. Jardine, T. L. Marsh, J. M. Tiedje, T. C. Hazen, and J. Zhou.** 2011. Dynamics of Microbial Community Composition and Function during In Situ Bioremediation of a Uranium-Contaminated Aquifer. Appl Environ Microbiol **77:**3860-3869.

16. **Wu, L., X. Liu, C. W. Schadt, and J. Zhou.** 2006. Microarray-based analysis of subnanogram quantities of microbial community DNAs by using whole-community genome amplification. Appl Environ Microbiol **72:**4931-4941.

17. **Wu, W. M., J. Carley, S. J. Green, J. Luo, S. D. Kelly, J. Van Nostrand, K. Lowe, T. Mehlhorn, S. Carroll, B. Boonchayanant, F. E. Lofller, D. Watson, K. M. Kemner, J. Z. Zhou, P. K. Kitanidis, J. E. Kostka, P. M. Jardine, and C. S. Criddle.** 2010. Effects of Nitrate on the Stability of Uranium in a Bioreduced Region of the Subsurface. Environ Sci Technol **44:**5104-5111.

18. **Wu, W. M., J. Carley, J. Luo, M. A. Ginder-Vogel, E. Cardenas, M. B. Leigh, C. C. Hwang, S. D. Kelly, C. M. Ruan, L. Y. Wu, J. Van Nostrand, T. Gentry, K. Lowe, T. Mehlhorn, S. Carroll, W. S. Luo, M. W. Fields, B. H. Gu, D. Watson, K. M. Kemner, T. Marsh, J. Tiedje, J. Z. Zhou, S. Fendorf, P. K. Kitanidis, P. M. Jardine, and C. S. Criddle.** 2007. In situ bioreduction of uranium (VI) to submicromolar levels and reoxidation by dissolved oxygen. Environ Sci Technol **41:**5716-5723.

19. **Zhou, J., S. Kang, C. W. Schadt, and C. T. Garten, Jr.** 2008. Spatial scaling of functional gene diversity across various microbial taxa. P Natl Acad Sci USA **105:**7768-7773.

20. **Zhou, J. Z., M. A. Bruns, and J. M. Tiedje.** 1996. DNA recovery from soils of diverse composition. Appl Environ Microb **62:**316-322.